Colloid Polym Sci 278:48–56 (2000)

ORIGINAL CONTRIBUTION

I. Voigt
F. Simon
H. Komber
H.-J. Jacobasch
S. Spange

Controlled synthesis of stable poly(vinyl formamide-*co*-vinyl amine)/silica hybrid particles by interfacial post-cross-linking reactions

Received: 28 June 1999
Accepted: 27 August 1999

I. Voigt · F. Simon (✉) · H. Komber
H.-J. Jacobasch (deceased)
Institute of Polymer Research,
Hohe Strasse 6,
D-01069 Dresden, Germany
e-mail: frsimon@ipfdd.de

I. Voigt · S. Spange (✉)
Department of Polymer Chemistry
Technical University Chemnitz Zwickau
Strasse der Nationen 62
D-09101 Chemnitz, Germany
e-mail:
stefan.spange@chemie.tu-chemnitz.de

Abstract The chemical synthesis and the physicochemical properties of stable poly(vinyl formamide-*co*-vinyl amine)/silica hybrid particles are presented. Copolymers of poly(vinyl formamide) (PVFA) and poly(vinyl amine) (PVAm) and their protonated forms were adsorbed onto silica from aqueous solutions. The influences of the pH strength and the ion concentration of the aqueous solution as well as the copolymer composition (degree of hydrolyzation of PVFA), and the molecular mass on the adsorption process were investigated by electrokinetic measurements, potentiometric titration, and quantitative elemental analyses. Silica surface-charge neutralization is achieved at a pH strength above 10 for highly hydrolyzed (95%) PVFA polymers. Decreasing the amino content in the PVAm chain shifts successively both the point of zero charge and the isoelectric point to lower pH values. PVFA-*co*-PVAm layers onto silica are adsorbed weakly. To fix these layers irreversibly, cross-linking reactions with (4,4′-diisocyanate)diphenyl methane were carried out on the surface of solid PVFA-*co*-PVAm/silica hybrid particles suspended in acetone. The cross-linking reaction, which is connected with the conversion of amino groups, is also a tool to control the surface charge of the PVFA-*co*-PVAm/silica hybrids. X-ray photoelectron spectroscopy and solid-state ^{13}C cross-polarization magic-angle spinning NMR spectroscopy were used to obtain information on the number of and the structure of the functionalized polyelectrolyte layers on silica. The success of cross-linking was also shown by the results of these spectroscopic methods.

Key words Polyelectrolyte adsorption · Silica · Hybrid materials · Copolymers from poly(vinyl formamide) and poly(vinyl amine) · Cross-linking

Introduction

The adsorption of polyelectrolytes onto various kinds of solid materials, for example, inorganic metal oxide particles, resins, flat surfaces, or fibers, is an intensively studied field of material research due to the practical relevance of polyelectrolyte in adhesion, flocculation, or wetting [1–4].

Recently, the efforts of several authors have been focused on the synthesis of stable layers which can be achieved by several preparation techniques [5–7]. Decher [5] developed a new technique for synthesizing stable polyelectrolyte multilayers consisting of various structurally different materials: oppositely charged polyelectrolytes were adsorbed consecutively, and so the surface charges altered after each adsorption step. Sukhorukov et al. [6] and Donath et al. [7] used similar techniques to synthesize novel polymeric hollow spheres. Poly(sodium styrene sulfonate), poly(allyl amino hydrochloride), poly(vinyl pyridine), and similar water-soluble polymers

[1–7] were often used for this purpose. Polymer/inorganic solid hybrid materials can also be synthesized by surface polymerization of suitable monomers on inorganic surfaces [8–12] or by applying the sol-gel technique [13–17].

Synthetic polyelectrolytes bearing quaternized ammonium or sulfonate groups are rather inert and are not very suitable for further chemical derivatization reactions under light conditions. Generally, it is of interest to functionalize chemically surface-fixed polyelectrolytes in order to improve their compatibility for biological or optical applications.

Poly(vinyl amine) (PVAm) is a potential polyelectrolyte candidate for a lot of applications for the following reasons. The primary amino groups of PVAm can be used for a lot of consecutive chemical derivatization reactions [18, 19]. Improved control of the ionic properties, for example, charge density and acid-base strength, is possible by simple proton adsorption because the charge carriers, commonly $-NH_3^+X^-$ groups, are directly located along the polymer backbone.

During the last few decades, various approaches to synthesize PVAm have been reported. Due to the fact that the vinyl amine monomer cannot be polymerized directly, PVAm was synthesized by modification reactions of suitable precursor polymers, for example polyacrylamide [20, 21], poly(vinyl acetamide) [22], poly(vinyl carbamate) [23], or poly(vinyl imide) [24]. For some of these polymer analogous reactions, rather rigorous reaction conditions are required and mostly a lot of disturbing side products and degradation of the polymers are observed.

A structurally well defined and water-soluble PVAm is available by an acid-catalyzed or base-catalyzed hydrolyzation reaction of poly(vinyl formamide) (PVFA) (Scheme 1) [18, 19]. High-molecular-mass products of PVFA are available by a radical polymerization of vinyl formamide [18, 19], whereas oligomeric products can be obtained by specific cationic polymerization reactions [25, 26]; therefore, the molecular mass of PVAm can be controlled over a wide range from M_n = 800 to 400,000 g mol^{-1}.

Furthermore, the charge density along the polymer backbone of PVAm can also be controlled by the degree

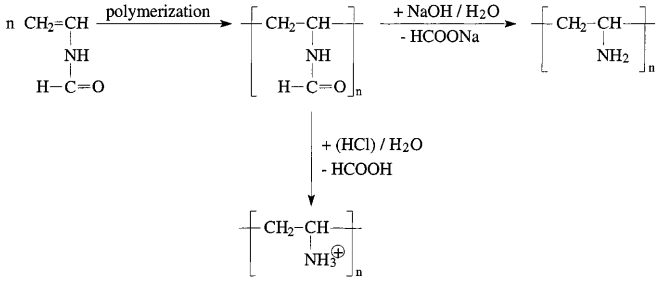

Scheme 1 Synthesis of poly(vinyl formamide) (*PVFA*)-*co*-poly(vinyl amine) (*PVAm*)

of hydrolyzation of the formamide groups. Therefore, it is expected that the use of poly(vinyl formamide-*co*-vinyl amine) (PVFA-*co*-PVAm), obtained exclusively from the monomer vinyl formamide, combined with appropriate inorganic solids is suitable to synthesize structurally well defined hybrid materials with quite different surface properties.

The present study reports the coating of silica particles with well-defined PVFA-*co*-PVAm in order to control the surface properties, such as charge density and acid–base characteristics, in water (Scheme 2). To fix the adsorbed PVFA-*co*-PVAm layers onto silica irreversibly, post-cross-linking reactions with the bifunctional isocyanate (4,4′-diisocyanate)diphenyl methane were carried out. It is expected that these reactions, which occur between adsorbed PVAm chains near the silica particle surface, transform the flexible polyelectrolyte layer into a more rigid one.

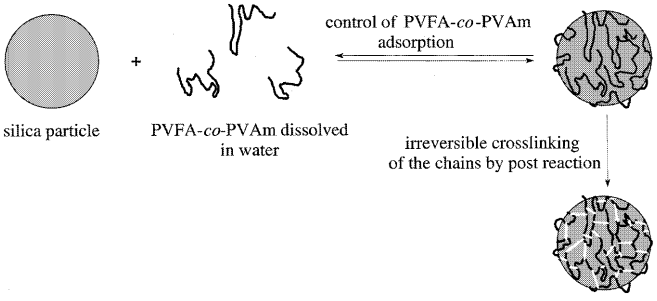

Scheme 2 Synthetic path towards stable PVFA-*co*-PVAm/silica hybrid particles

Methods characterizing the state of equilibrium between solid particles and surrounding aqueous media, such as potentiometric titration and electrokinetic measurements, were used to observe the adsorption process of PVFA-*co*-PVAm samples with different molecular masses (M_n = 1,000, 40,000, and 400,000 g mol^{-1}) and the degree of PVFA hydrolyzation. Using these data, changes in surface charge densities and acid–base properties are discussed. In addition, X-ray photoelectron spectroscopy (XPS) and solid-state ^{13}C cross-polarization magic-angle spinning (CPMAS) NMR spectroscopy were applied to study the molecular build-up of the hybrid materials and the interfacial region between the inorganic solid and the adsorbed polyelectrolyte layer.

Experimental

Materials

Kieselgel 60 (Merck, Darmstadt, Germany), a commercially available spherical silica, was used as the inorganic substrate material. The main diameter of the silica particles ranged between 20 and 40 μm. Kieselgel 60 particles are microporous. The

distribution of the pore diameters has a maximum in the range between 40 and 60 Å. This means that the majority of the pores are inaccessible to the polyelectrolyte molecules but are accessible to small ions.

The PVFA-*co*-PVAm with different molecular weights [M_n = 1,000 g mol^{-1} (A), 40,000 g mol^{-1} (B), and 400,000 g mol^{-1} (C)] were kindly provided by BASF (Ludwigshafen, Germany). The precursor oligomer of sample A was synthesized by cationic polymerization of VFA with iodine as an initiator [26]. To synthesize samples B and C, VFA was polymerized radically [18, 19]. PVFA-*co*-PVAm polyelectrolytes containing different numbers of amino groups were obtained by partial acid hydrolyzation of the corresponding precursor oligomers with hydrochloric acid [25].

For the experiments, 30% (PVFA-*co*-PVAm-30), 48% (PVFA-*co*-PVAm-48), and 95% (PVFA-*co*-PVAm-95), of all formamide groups in the PVFA chain were hydrolyzed. The degree of hydrolyzation was determined by ^{1}H NMR spectroscopy [18, 19]. The formation of block copolymers during the hydrolyzation procedure can be excluded .

The commercially available (4,4′-diisocyanate)diphenyl methane (Merck, Darmstadt, Germany) was used as received.

Adsorption procedure

PVFA-*co*-PVAm samples were dissolved in aqueous KCl solutions of different ionic strength. Then, 0.5 g silica was suspended in 100 ml PVFA-*co*-PVAm solution. The adsorption equilibrium was reached after 24 h. During the adsorption process, the suspension was shaken gently at 25 °C. The modified particles were filtered off with the help of slight suction. The hybrid materials were washed carefully with distilled water and dried at room temperature for 12 h.

Cross-linking with (4,4′-diisocyanate)diphenyl methane

The cross linking reactions were carried out using the PVFA-*co*-PVAm/silica hybrid particles and (4,4′-diisocyanate)diphenyl methane as a coupling agent. For this, the hybrid particles were suspended in pure acetone. Then, 0.01 w/w% (weight per weight percent with respect to silica) (4,4′-diisocyanate)diphenyl methane dissolved in acetone was added. The suspension was shaken gently at 35 °C for 3 h. After filtering and washing the hybrid particles with acetone, they were dried for 12 h at room temperature.

Solid-state NMR spectroscopy

The ^{13}C CPMAS spectra were obtained using a Bruker AMX 300 spectrometer operating at 75.47 MHz for ^{13}C. The samples were spun at 4–5 kHz in a 7-mm CPMAS probe head (Bruker) at room temperature. The spectra were referenced using the CH signal of external atamantane at 38.6 ppm. The experiments were performed with 5 μs ^{1}H 90° pulse duration, a contact time of 1 ms, and a recycle delay of 2 s.

X-ray photoelectron spectroscopy

XPS measurements were carried out by means of an ESCAlab 220i spectrometer (Vacuum Generator, England) equipped with a non-monochromatized Mg K_α X-ray source. The binding energies were adjusted using the Au $4f_{7/2}$ peak at 84.00 eV and the Cu $3d_{5/2}$ peak at 932.67 eV [27]. An electron-flood gun to eliminate sample charging was not used. The kinetic energy of the photoelectrons was determined by means of a hemispherical analyzer with a constant-pass energy of 80 eV for survey spectra and of 25 eV for high-resolution spectra.

All spectra were adjusted to the hydrocarbon reference peak C 1*s* at 285.00 eV [28]. The quantitative elemental compositions were determined from the peak area using Wagner's sensitivity factors [29] and the spectrometer transmission function. Normalized peak areas are denoted in brackets, for example, [N]. The inelastic spectrum background was subtracted according to Shirley's procedure [30].

The high-resolution spectra were deconvoluted into different component peaks. The parameters of each component peak were its binding energy, peak area, full width at half-maximum, and Gaussian–Lorentzian ratio.

Electrokinetic measurements

For microelectrophoresis experiments using the ZetaSizer III (Malvern Instruments) dilute suspensions (0.01 g ml^{-1}) of the hybrid particles in KCl solutions of different pH values ($3 \geq pH \geq 10$) were prepared. The pH values were adjusted with HCl and KOH. During all microelectrophoresis measurements the electrical field strength was 100 V cm^{-1}.

The value of the electrokinetic potential (zeta potential) was calculated from the measured electrophoretic mobility according to Smoluchowski's equation [31].

Potentiometric titrations

Potentiometric titrations were carried out by means of an automatic titration setup at 25 °C. Before starting the titration, suspensions of 0.3 g hybrid material in 60 ml water or KCl solutions were purified with nitrogen for 30 min. The suspensions were titrated between pH 3 and 10 using 0.1 mol l^{-1} KOH and 0.1 mol l^{-1} HCl. Titrations in the absence of silica and hybrid materials were performed in order to correct the surface charge values.

Results and discussion

Bare silica surface

Silica particles suspended in water or in an aqueous solution may be considered as a polyelectrolyte. The surface charging of the silica particles is either the result of dissociation processes of Brønsted-acidic silanol groups (Si-OH) forming negatively charged silanolate ions (Si-O$^-$) or proton adsorption yielding Si-OH$_2^+$ species. In a wide pH range the two charge generation mechanisms may take place simultaneously on the silica surface because the acidity of surface silanol groups can be quite different [32]. PVFA-*co*-PVAm molecules also have discrete charges in their chain; therefore, an important component of the driving force of PVFA-*co*-PVAm adsorption onto silica surfaces should be the Coulomb force between the charge centers of the solid surfaces and the PVFA-*co*-PVAm chains. The interaction of components with the oppositely charged groups advances the adsorption process, while components having the same polarity do not favor adsorption. Therefore, to understand the adsorption behavior of PVFA-*co*-PVAm onto silica powder particles it is necessary to know the net charging of silica surfaces in water and in the aqueous KCl solutions which were used as solvents for PVFA-*co*-PVAm.

Microelectrophoretic experiments in water show that the zeta-potential values are positive in the range pH < 3. This indicates a preferred adsorption of protons forming $Si\text{-}OH_2^+$ groups. At pH 3.0 the isoelectric point (IEP) is observed. A further increase in pH decreases the zeta-potential values. Then, the dissociation reactions form negatively charged silanolate ions on the silica surface. At a pH of about 9 all accessible Si-OH groups are dissociated. The zeta-potential values remain constant.

Here, it is necessary to note that the zeta-potential values determined from experiments in pure water do not depend only on pH: they are also influenced by the ionic strength of the aqueous media. The variation of the pH over a range between 3 < pH < 10 also changes the ionic strength of the aqueous media significantly. Consequently, the electrokinetic measurements were repeated using aqueous KCl solutions of different concentrations. Furthermore, it is well known that the ionic strength of the aqueous salt solution controls the conformation of flexible polyelectrolyte molecules and influences their adsorption behavior.

The increase in the ionic strength in the aqueous KCl solutions leads to an enhancement of the compression of the electrochemical double layer. Therefore, smaller zeta-potential values are observed with increasing ionic strength; however, the shape of the curves and the IEPs are not influenced by the KCl concentration (Fig. 1). This indicates that only protons (H^+) and hydroxyl (OH^-) ions are potential-determining ions, whereas K^+ and Cl^- act as inert ions.

From the pH dependence of the zeta potential the Brønsted acidity of the silica surface can be determined by means of a modified Gouy–Chapman–Stern–Graham model described in Ref. [32]. The adsorption molar free energies of OH^- ions of the most acidic surface centers were found to be $\Phi_{OH^-} = -64.7$ to -57.9 kJ mol^{-1} depending on the ionic strength of the KCl solutions. The corresponding pK_a values were pK_a = 4.4–5.6. That means that the bare silica surface used is a moderately strong Brønsted acid in aqueous media. The values found for Kieselgel 60 are a little bit higher than values found for other silica by Sidorova et al. [33] and Simon et al. [32].

The surface charge densities of pure silica were determined by means of potentiometric titrations at different KCl concentrations. Figure 2 shows that the surface density increases steadily with increasing pH.

Independent of the setups used for electrokinetic or potentiometric measurements the charge generation mechanisms of silica particles suspended in aqueous solution have to be the same. Nevertheless, the curves of the potentiometric experiments do not show any approaches to the plateau region observed in electrokinetic experiments at pH > 9. In contrast the functions $\sigma = \sigma(\text{pH})$ show the steady slope of an exponential function. In the electrokinetic experiments the silanol groups in the pores of silica do not contribute significantly to the zeta-potential value; however, during the titration the silanol groups of the inner surface are included.

Adsorption behavior of PVFA-*co*-PVAm onto silica surfaces

The degree of hydrolyzation of the formamide groups as well as the molecular mass of the PVFA-*co*-PVAm samples strongly affect their adsorption behavior from aqueous solutions onto silica surfaces.

The influence of the degree of hydrolyzation on the adsorption behavior is discussed for PVFA-*co*-PVAm samples with a molar mass of M_n = 400,000 g mol^{-1}.

Figure 3 shows the survey photoelectron spectra of bare silica (Fig. 3 trace a) and of a PVFA-*co*-PVAm-95/silica hybrid material (Fig. 3 trace b). Clearly, it can be seen that the bare silica does not contain considerable amounts of carbon (C 1*s*) and nitrogen (N 1*s*). After the adsorption of PVFA-*co*-PVAm the amounts of carbon as well as nitrogen increase significantly. The atomic ratio found experimentally to be $[N]:[C]_{exp}$ = 0.473 is close to the theoretically expected ratio of

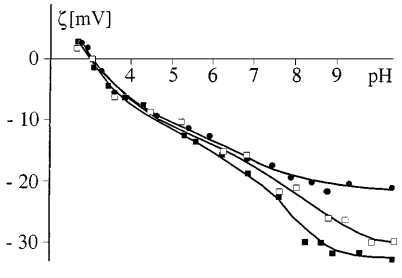

Fig. 1 Dependence of the zeta-potential of bare Kieselgel 60 on pH and ionic strength: measured in pure water (■), measured in 1×10^{-3} mol l^{-1} KCl (□), measured in 1×10^{-2} mol l^{-1} KCl (●), measured in 1×10^{-1} mol l^{-1} KCl (○)

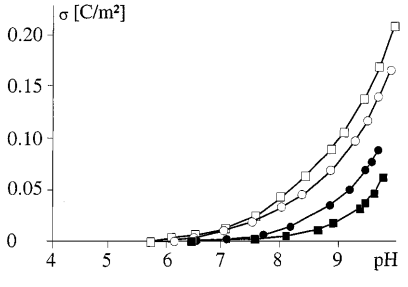

Fig. 2 Dependence of the surface charge, σ, of bare Kieselgel 60 on pH and ionic strength: measured in pure water (□), measured in 1×10^{-3} mol l^{-1} KCl (○), measured in 1×10^{-2} mol l^{-1} KCl (●), measured in 1×10^{-1} mol l^{-1} KCl (■)

$[N]:[C]_{theo}$ = 0.488. This indicates that the C 1*s* as well as the N 1*s* peak are caused by the adsorbed polyelectrolyte.

The high-resolution C 1*s* spectrum of the PVFA-*co*-PVAm-95/silica hybrid material supports the above assumption. The spectrum was deconvoluted into three component peaks (Fig. 4a). Component peak A represents the hydrocarbon species C_xH_y. The second component peak (B) is shifted by 0.93 eV to higher binding energies. It reflects the presence of C-NH_2 as well as C-NH-C(H)=O bonds [28]. A third component peak (C) was found at 288.72 eV. This component peak appears from the presence of the HN-C(H)=O formamide groups of PVAF. The ratio of the component peak areas C:B = 0.041 is in a rather good agreement with the expected value at a degree of hydrolyzation of 95% determined by ^{1}H NMR spectroscopy of PVFA-*co*-PVAm-95 [18, 19].

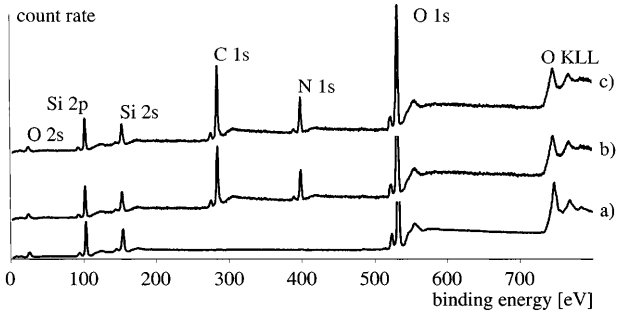

Fig. 3 Survey photoelectron spectra of bare silica (*a*), PVFA-*co*-PVAm-95 (M_n = 400,000 g mol^{-1}) adsorbed onto silica (*b*) and PVFA-*co*-PVAm-95 after cross-linking with (4,4′-diisocyanate)diphenyl methane on silica (*c*)

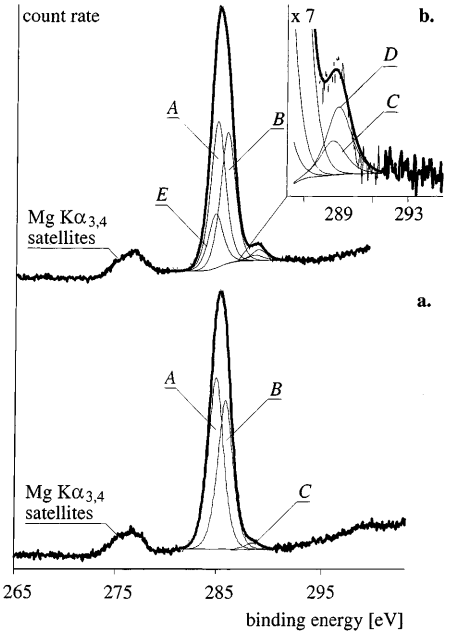

Fig. 4 C 1*s* photoelectron spectra of **a** PVFA-*co*-PVAm-95 (M_n = 400,000 g mol^{-1}) adsorbed onto silica (*a*) and **b** PVFA-*co*-PVAm-95 after cross-linking with (4,4′-diisocyanate)diphenyl methane on silica

If we assume that the N 1*s* peak appears only from the polyelectrolyte layer and that the Si 2*p* peak is a specific signal of the substrate material, the [N]:[Si] atomic ratio should be an accurate measure of the amount of adsorbed polyelectrolyte. The polyelectrolyte layers are laterally inhomogeneous; therefore, it can be assumed that the amount of Si is not influenced significantly by the amount of adsorbed polyelectrolyte. Furthermore, the amount of nitrogen in PVFA-*co*-PVAm does not depend on the degree of hydrolyzation (Scheme 1).

The dependence of the amount of PVFA-*co*-PVAm adsorbed on the degree of hydrolyzation is shown in Fig. 5. If PVFA-*co*-PVAm samples containing a low number of amino groups are used, the amount of polyelectrolyte absorbed cannot be improved significantly by modification of the experimental conditions. It is striking that the amount of PVFA-*co*-PVAm adsorbed is strongly increased by using a sample with a degree of hydrolyzation of 95%. These results show that specific interactions, which are caused by coordinatively induced chemical bonds between the silica surface and former PVAF segments of the PVFA-*co*-PVAm chains, are of minor importance. Therefore, it can be concluded that the degree of adsorption is attributed to electrostatic forces between the oppositely charged SiO^- and -NH_3^+ groups.

Consistent results were obtained from electrokinetic studies of hybrid particles made from silica and differently hydrolyzed PVFA-*co*-PVAm (Fig. 6).

The adsorption of the precursor polymer PVFA (considered as a "uncharged" reference sample of PVFA-*co*-PVAm) onto silica does not influence significantly the shape of silica's $\zeta = \zeta(pH)$ function; however, the shift in the IEP from pH = 3 to 5 indicates that silanol groups are involved in the adsorption process. It is assumed that these silanol groups are

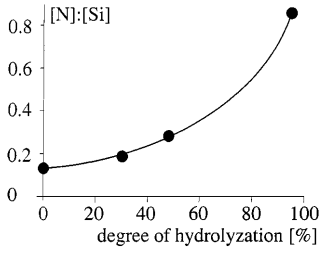

Fig. 5 Influence of the degree of hydrolyzation of the PVFA sample with M_n = 400,000 g mol^{-1} on the amount of adsorbed polyelectrolyte as measured by X-ray photoelectron spectroscopy (*XPS*)

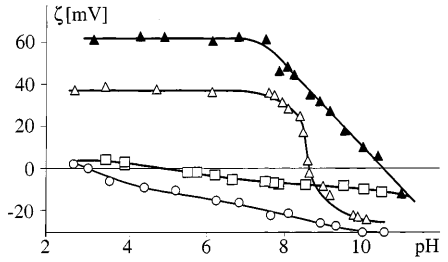

Fig. 6 Influence of the degree of hydrolyzation of the PVFA sample with M_n = 400,000 g mol^{-1} on the zeta-potential as a function of pH, compared to bare silica measured in 1×10^{-3} mol l^{-1} KCl at 25 °C: bare silica (○), PVFA (M_n = 400,000 g mol^{-1}) (□), PVFA-*co*-PVAm-30 (△), PVFA-*co*-PVAm-95 (▲)

shielded by co-ordinatively bound PVFA segments or that they participate in hydrogen-bridge linkages with the polyelectrolyte molecules. Proton-transfer reactions from silanol groups to the PVFA molecules are not expected, because PVFA does not contain any amino groups. The covering of the most acidic silanol groups by PVFA decreases the Brønsted acidity of the silica surface to p$K_a \approx 7$. The hydrolyzation of 30% of the formamide groups and the simultaneous introduction of protonable amino groups of the adsorbed polymer change the ζ–pH plot to a typical shape indicating Brønsted-base surface properties [34]. The presence of protonated amino groups results in positive zeta-potential values over a wide pH range up to IEP = 8.8. The pK values, pK_a = 8.5 and its corresponding pK_b = 5.5, determined from the Gouy–Chapman–Stern–Graham model [32] quantify the moderate base strength of the PVFA-*co*-PVAm-30/silica hybrid surface. The hybrid surface basicity increases with the progress of hydrolyzation of formamide groups. The PVFA-*co*-PVAm-95/silica hybrid material with pK_b = 4.9 exhibits strong Brønsted-base properties.

The different graphs in Fig. 6 show that it is possible to use the degree of hydrolyzation of PVFA-*co*-PVAm to control and predict the surface acidity or basicity of solid surfaces over a wide pH range.

Despite the positive zeta-potential values of the PVFA-*co*-PVAm-30/silica hybrid material over a pH range from 5.5 < pH < 8.8 the corresponding surface charge densities calculated from the results of potentiometric titrations are negative (Fig. 7).

According to the results shown in Fig. 7, it is not possible to compensate for the negative surface charge of silica completely by the adsorption of PVFA-*co*-PVAm-30 or PVFA-*co*-PVAm-48. The PVFA-*co*-PVAm chains with a rather low degree of hydrolyzation are only suitable for adsorption onto a few sites of the silica surface; hence, a tail or a wide-loop conformation of the PVFA-*co*-PVAm chains should dominate. However, the polyelectrolyte tails and loops, which carry positive charges, do not only cause the positive potential in the shear plane (zeta-potential). The polyelectrolyte layer thickness also controls the average distance between the shear plane and the rigid silica surface. A high number of tail and wide-loop conformations shifts the shear plane to higher distances from the rigid silica surface and decreases the zeta-potential. In contrast, a polyelectrolyte having a higher fraction of a train conformation does not influence the shear plane position strongly.

The specific behavior, negative surface charge densities versus positive zeta-potential values, was only observed for PVFA-*co*-PVAm/silica particles with PVFA-*co*-PVAm components bearing less than 50% of hydrolyzed formamide groups (Figs. 7, 8). The higher number of amino groups as a result of the progress of the hydrolyzation of formamide groups increasess the number of positively charged ammonium groups in the polyelectrolyte chain. That means, the polyelectrolyte molecule has more suitable sites to interact with the oppositely charged surface centers of silica. The enormous number of interacting sites shifts the tail/loop number of adsorbed PVFA-*co*-PVAm chains to a higher number of train conformations. As a result a more closely packed polyelectrolyte layer is built up onto the silica surface and shields it. This is illustrated by the adsorption experiment where PVFA-*co*-PVAm-95 was adsorbed onto silica. Figure 8 shows that the higher degree of hydrolyzation leading to a higher number of

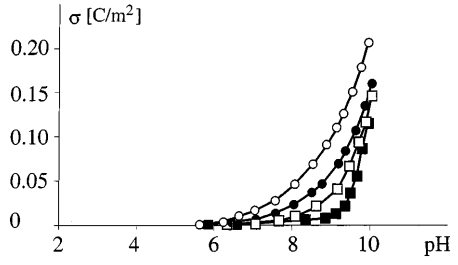

Fig. 7 Dependence of the surface charge, σ, of PVFA-*co*-PVAm-30/silica hybrid material on pH and ionic strength: measured in pure water (■), measured in 1×10^{-3} mol l^{-1} KCl (□), measured in 1×10^{-2} mol l^{-1} KCl (●), measured in 1×10^{-1} mol l^{-1} KCl (○)

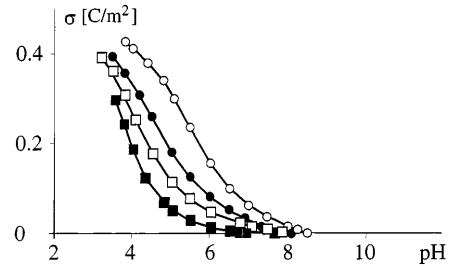

Fig. 8 Dependence of the surface charge, σ, of PVFA-*co*-PVAm-95/silica hybrid material on pH and ionic strength: measured in pure water (■), measured in 1×10^{-3} mol l^{-1} KCl (□), measured in 1×10^{-2} mol l^{-1} KCl (●), measured in 1×10^{-1} mol l^{-1} KCl (○)

protonable amino groups changes the sign of the surface charge density in the pH range pH < 8.5 to positive.

The results show that train, loop, and tail conformations of adsorbed PVFA-*co*-PVAm chains can contribute to the particle surface structure depending on the degree of charge localization along the PVFA-*co*-PVAm chain. According to the experimental findings, presumed structures of PVFA-*co*-PVAm adsorbed onto silica are drawn in Scheme 3.

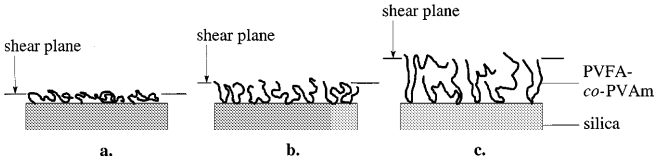

Scheme 3 Proposed PVFA-*co*-PVAm conformations on silica surfaces as a function of the number of -NH_3^+ charge carriers in the polyelectrolyte chain. *a* PVFA-*co*-PVAm-95, *b* PVFA-*co*-PVAm-48, *c* PVFA-*co*-PVAm-30

The adsorption behavior of PVFA-*co*-PVAm from aqueous solutions onto silica is not only determined by the degree of hydrolyzation of the PVFA but also depends on the molecular mass of the polyelectrolyte samples.

The influence of the molecular mass on the adsorbed PVFA-*co*-PVAm-95 fraction, shown in Fig. 9, is detectable, in particular for pure aqueous solutions which do not contain KCl. Here, the amount of adsorbed PVFA-*co*-PVAm increases significantly with increasing molecular weight of PVFA-*co*-PVAm; however, in cases of adding certain amounts of KCl to the aqueous solutions the effect of the molecular weight on the adsorption behavior is not clearly detectable.

The decrease in the amount adsorbed on increasing the salt concentration is in contrast to results obtained for the adsorption of poly(diallyl dimethyl ammonium chloride) onto different silica samples [35, 36]. Probably, the chloride ions shield the segment–segment interactions between charged groups inside the coil of an individual polyelectrolyte chain as well as the interaction between the polyelectrolyte chain and the silica surface [37–40]. This explanation is also consistent with the assumption that electrostatic forces determine the adsorption mechanism of PVFA-*co*-PVAm chains to silica explained previously.

From the adsorption experiments it can be concluded that the surface and interphases of the PVFA-*co*-PVAm/silica hybrids have different properties depending on the degree of hydrolyzation of PVFA, the molecular mass, as well as the salt concentration. Knowledge of these factors is of importance in order to make use of the PVFA-*co*-PVAm/silica hybrid particles.

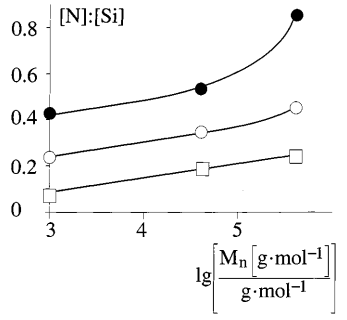

Fig. 9 Influence of the molecular weight on the amount of adsorbed PVFA-*co*-PVAm-95 measured by XPS and indicated by [N]:[C] ratios. Adsorption experiments were carried out at pH 9: adsorption carried out in pure water (●), adsorption carried out in1×10^{-2} mol l^{-1} KCl (○), adsorption carried out in 5×10^{-2} mol l^{-1} KCl (□)

However, it is even expected that the stability of PVFA-*co*-PVAm layer adsorbed onto silica can be disturbed by treating the particles with salt solutions or various acids and bases. For this reason the irreversible fixing of adsorbed PVAm chains is required to improve the application of PVFA-*co*-PVAm/silica hybrid particles in aqueous media.

Chemical cross-linkage of adsorbed PVFA-*co*-PVAm

Postchemical reactions of accessible amino groups of adsorbed PVFA-*co*-PVAm chains with suitable reagents cause the introduction of novel functional groups and the reduction in interaction forces between the polymer layer and the silica surface.

To cross-link PVFA-*co*-PVAm chains the commercially available reagent (4,4′-diisocyanate)diphenyl methane was used. It was expected that the adsorbed PVFA-*co*-PVAm chains would become irreversibly linked to the particle surface. The formation of a two-dimensional network is desired to cover each single particle effectively. Agglomeration reactions occurring between the PVFA-*co*-PVAm chains should be avoided. The cross-linking was carried out in a two-step synthesis. In the first step PVFA-*co*-PVAm was adsorbed from an aqueous solution as described previously. In the second step a post-cross-linking reaction was carried out on the separated particles using (4,4′-diisocyanate)diphenyl methane dissolved in acetone (Experimental).

Principally, the two isocyanate groups of (4,4′-diisocyanate)diphenyl methane can react with amino groups of the PVFA-*co*-PVAm chains as well as with silanol groups of the silica surface. Qualitative structural analysis of particles modified with (4,4′-diisocyanate)diphenyl methane was carried out by means of ^{13}C CPMAS NMR spectroscopy (Fig. 10a, b).

Figure 10a shows the ^{13}C CPMAS spectrum of PVFA-*co*-PVAm-95/silica hybrid particles. Besides the broad signal of the main chain CH and CH_2 groups at about 46 ppm appearing from the adsorbed polyelectrolyte layer an additional signal is observed at 165.2 ppm. This signal is caused by the carbonyl carbons of formamide groups remaining from the parent PVFA. The spectrum of this sample after reaction with (4,4′-diisocyanate)diphenyl methane is shown in Fig. 10b. New signals in the aromatic carbon region (138.0, 128.9, and 119.2 ppm) and an enhanced shoulder at 41 ppm are due to the diphenyl methane unit. The signal of the isocyanate group at about 125 ppm could not be detected; however, a new broadened carbonyl signal appears at 158.5 ppm. This chemical shift is expected for urethane and urea linkages [41]. This signal can also be observed for a reaction product of pure PVAm and (4,4′-diisocyanate)diphenyl methane. Obviously, it is caused by the urea linkage between the PVAm backbone and the diphenyl methane unit, indicating the post-cross-linking reaction. Signals of a linkage between silanol groups and (4,4′-diisocyanate)diphenyl methane are not detectable.

XPS was also used for the quantitative assignment of the structure elements. Figure 3c shows the survey photoelectron spectrum of a PVFA-*co*-PVAm-95/silica hybrid material after post-cross-linking compared with spectra taken from bare silica and PVFA-*co*-PVAm-95/silica hybrid material without cross-linked structures. After the post-cross-linking reaction of PVFA-*co*-PVAm-95 with (4,4′-diisocyanate)diphenyl methane, the relative amount of carbon is evidently increased. [N]:[C] decreases from 0.4726 to 0.3141. The [Si]:[O] ratio is indeed weakly influenced by the cross-linking process. It increases from 0.38 (PVFA-*co*-PVAm-95/silica) to 0.39 (PVFA-*co*-PVAm-95/silica cross-linked).

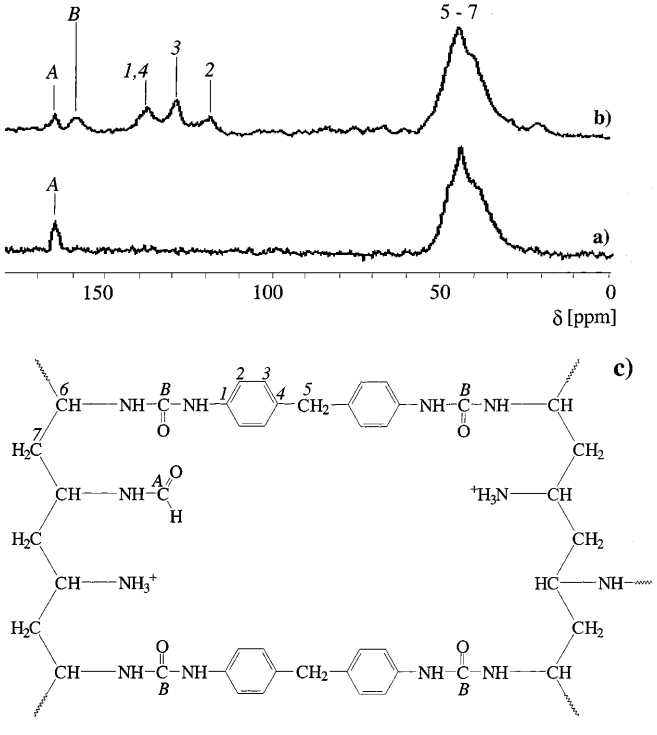

Fig. 10 Solid-state ^{13}C cross-polarized magic-angle spinning (*CPMAS*) NMR spectra of PVFA-*co*-PVAm-95/silica hybrid particles (M_n = 400,000 g mol^{-1}) **a** before cross-linking and **b** after cross-linking with (4,4′-diisocyanate)diphenyl methane **c** Virtual structure of a (4,4′-diisocyanate)diphenyl methane functionalized PVFA-*co*-PVAm network cut out and assignment of the signals in the ^{13}C CPMAS NMR spectra

The C 1*s* spectrum of the cross-linked PVFA-*co*-PVAm-95 layer adsorbed onto silica is shown in Fig. 4b. It is similar to the C 1*s* spectrum of non-cross-linked PVFA-*co*-PVAm-95/silica hybrid material; however, in Fig. 4b the peak widths of the main peak and the shoulder at about 288 eV are wider. Therefore, the spectrum was deconvoluted into five component peaks. The component peaks A, B, and C represent the same structural elements discussed for the non-cross-linked PVFA-*co*-PVAm-95/silica hybrid. The new component peak E at 284.7 eV appears from carbon atoms of the phenyl ring of (4,4′-diisocyanate)diphenyl methane. Component peak D at 289.03 eV shows the presents of urea groups [28] formed by the cross-linking reaction of amino groups and isocyanate groups.

The area ratio [D]:[E] = 0.1933 found experimentally is close to the expected ratio of 0.2. It shows that both isocyanate groups of (4,4′-diisocyanate)diphenyl methane are able to react and cross-link the PVFA-*co*-PVAm-95 chains successfully. The introduction of two additional amino groups and only one saturated hydrogen-bonded carbon atom per (4,4′-diisocyanate)diphenyl methane molecule increases the [B]:[A] ratio slightly, while [C]:[A] is nearly constant.

Results of electrokinetic measurements of PVFA-*co*-PVAm-95/silica hybrid particles cross-linked with different amounts of (4,4′-diisocyanate)diphenyl methane are shown in Figure 11.

The post-cross-linking reaction of the amino groups of the PVFA-*co*-PVAm layer with the isocyanate groups of (4,4′-diisocyanate)diphenyl methane decreases the number of protonable amino groups in the PVFA-*co*-PVAm chains. As expected, with increasing amount of cross-linking agent, corresponding to increased conversion of amino groups, the IEP of the hybrid particles surface shifts to lower pH values. Of course, the decrease in the number of positive charge carriers in the polyelectrolyte layer results in a decrease in number of the electrostatic interactions between the negatively charged silica surface centers and polyelectrolyte molecules. Advantageously, the limitation of electrostatic interactions of the polyelectrolyte layer cannot be removed because the cross-linking process forms a network like a cage covering the silica particle.

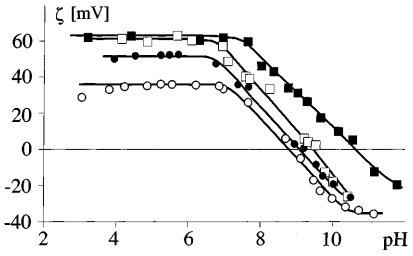

Fig. 11 Dependence of the zeta-potential of PVFA-*co*-PVAm-95/silica particles functionalized with different amounts of (4,4′-diisocyanate)diphenyl methane on pH values measured in an aqueous 1×10^{-3} mol l^{-1} KCl at 25 °C: nonfunctionalized PVFA-*co*-PVAm-95/silica particles (■), 0.01 w/w% (4,4′-diisocyanate)diphenyl methane (□), 0.05 w/w% (4,4′-diisocyanate)diphenyl methane (●), 0.10 w/w% (4,4′-diisocyanate)diphenyl methane (○) w/w% = weight of (4,4′-diisocyanate)diphenyl methane per gram PVFA-*co*-PVAm-95/silica ×100%

Despite the transformation of a certain number of amino groups into urea groups, the qualitative shape of the zeta-potential plots as a function of pH is not changed significantly. That indicates that PVFA-*co*-PVAm can be used as a precursor polymer for the gradual functionalization of silica particles and other Brønsted-acidic surfaces with amino functionalities. Postchemical reactions of PVFA-*co*-PVAm/silica particles with isocyantes or other electrophilic reagents offer a wide field of applications because of the simple experimental procedure, this material combination seems promising for the construction of tailor-made polyelectrolyte networks on Brønsted-acidic surfaces or for other multicomponent systems.

Acknowledgements This research was gratefully supported by the DFG "Polyelectrolyte mit definierter Molecülarchitektur". The authors also wish to thank BASF Aktiengesellschaft (Ludwigshafen, Germany) for the kind gift of the poly(vinyl formamide-*co*-vinyl amine) samples, financial support, and scientific cooperation.

References

1. Dautzenberg H, Jaeger W, Kötz J, Philipp B, Seidel C, Stscherbina D (1994) Polyelectrolytes: formation, characterization and application, Carl Hanser, Munich
2. Bauer D, Killmann E, Jaeger W (1998) Prog Colloid Polym Sci 109:161
3. Huguenard C, Widmaier J, Elaissari A, Pefferkorn E (1997) Macromolecules 30:1434
4. Gailliez-Degremont E, Bacquet M, Laureyns J, Morcellet M (1997) J Appl Polym Sci 65:871
5. Decher G (1997) Science 227:1232, and references therein
6. Sukhorukov GB, Donath E, Lichtenfels H, Knippel E, Knippel M, Möhwald H (1998) Colloids Surf A 137:253
7. Donath E, Sukhorukov GB, Caruso F, Davis SA, Möhwald H (1998) Angew Chem 110:2324 and references therein
8. Spange S, Eismann U, Langhammer E, Höhne S (1997) Macromol Symp 126:223
9. Spange S, Simon F, Heublein G (1991) J Macromol Sci P. & A. Chemistry A 28:373
10. Spange S, Simon F, Schütz H, Schramm A, Winkelmann H (1992) J Macromol Sci P. & A. Chemistry A 29:997
11. Rühe J (1994) Nachr Chem Tech Labor 42:1237
12. Rühe J (1997) Macromol Symp 126:215
13. Miksa B, Slomkowski S (1995) Colloid Polym Sci 273:47
14. Hotz J, Meier W (1998) Langmuir 14:1031
15. Rojas OJ, Claesson PM, Muller D, Neuman RD (1998) J Colloid Interface Sci 205:77
16. Jordan R, Graf K, Riegler H, Unger KK (1996) Chem Commun 1025
17. Shi Y, Seliskar J (1997) Chem Mater 9:821
18. Pinschmidt RK, Renz WL, Caroll WE, Yacouth K, Drescher J, Nordquist AF, Chen N (1997) J Macromol Sci Pure App Chem A 34:1885
19. Badesso RJ, Nordquist AF, Pinschmidt RU, Sagl DJ (1996) Adv Chem Ser 248:489
20. Tanaka H (1979) J Polym Sci Polym Chem Ed 17:1239
21. Achari AE, Coqueret X, Lablache-Combier A, Loucheux C (1993) Makromol Chem 194:1879
22. Dawson DJ, Gless RD, Wingward RE (1976) J Am Chem Soc 98:5996
23. Hart R (1959) Makromol Chem 32:51
24. Bayer E, Geckeler K, Weingartner K (1980) Makromol Chem 181:585
25. Spange S, Madl A, Eismann U, Utecht J (1997) Macromol Rapid Commun 18:1075
26. Madl S, Spange S, Waldbach T, Anders E, Mahr N (1999) Macromol Chem Phys 200:1495
27. Anthony MT, Seah MP (1984) Surf Interface Anal 6:107
28. Beamson G, Briggs D (1990) High Resolution XPS of Organic Polymers. Wiley, Chichester
29. Wagner CD, Davis LE, Zeller MW, Taylor JA, Raymond RH, Gale LH (1981) Surf Interface Anal 3:211
30. Shirley DA (1972) Phys Rev B B5:4709
31. Nitzsche R, Simon F (1997) Techn Messen Sensoren Geräte Syst 64:106
32. Simon F, Jacobasch HJ, Spange S (1998) Colloid Polym Sci 276:930
33. Sidorova MP, Lyklema J, Fridrichsberg DA (1976) Kolloids Zh 38:716
34. Jacobasch HJ, Grundke K, Schneider S, Simon F (1995) J Adhes 48:57
35. Bauer D, Killmann E (1997) Macromol Symp 126:173
36. Rehmet R, Killmann E (1999) Colloids Surf A 149:323
37. Van de Steeg HGM (1992) Langmuir 8:2538
38. Durand G, Lafuma F, Audebert R (1988) Prog Colloid Polym Sci 76:278
39. Wang T, Audebert R (1988) J Colloid Interface Sci 121:32
40. Davies RJ, Dix L, Toprakcioglu C (1989) J Colloid Interface Sci 129:145
41. Kaji A, Arimatsu Y, Murano M (1992) J Polym Sci Part A Polym Chem 30:287